

# DIGITAL IMAGE ENHANCEMENT AND PROCESSING IN MACHINING

<sup>1</sup>Vibhash S. Sisodia, <sup>2</sup>Lalit Kr. Tyagi, <sup>3</sup>Shashi Kr. Singh, <sup>4</sup>Ram Singh

Research Scholars, JIT University, Rajasthan & Singhania University, Rajasthan-INDIA

## ABSTRACT

*This paper presents a new approach for measurement and defect detection of mechanical parts using Machine vision and image processing. It has an advantage over traditional method where the surface geometry is not touched and line to line scanning is not required. In this system, a CCD camera is used to grab the image of the sample using optical set up along with image processing software and hardware. This paper explains how 3D parameters can be measured to provide greater insight into surface finish. It also includes two cases in which 3D parameters measurements are essential in the design and development of high performance surfaces. Experimental results demonstrated good correlation between the received signal parameters and the root mean square surface roughness. The defects are detected and measured up to 0.1 micro meter.*

## INTRODUCTION

The measurement of surface roughness is important in areas of optics such as mirrors used in laser gyro systems, diamond turned optics, contact lenses, optical disks, soft lenses, contact lenses, polygon scanners and optical fibers. Surface roughness characterization is also of much interest in the magnetic storage area where the roughness of magnetic tape, floppy disks, hard disks, and magnetic heads is very important. There are two basic methods to measure the roughness of a surface (i) optical method (ii) mechanical method.

Mechanical methods are based on the principle of profilometers. These are very expensive and unstable devices. The main disadvantage of these devices is the contact with the surface, which could scratch the surface and the device could give inaccurate readings of the roughness measurement. The other method is optical based, non-contact and is superior in many ways like very fast and complete scanning and processing in one go

The present technique is based on optical phenomena principles, which are used to measure roughness. Realization of these methods is inexpensive and does not require any high precision and sophisticated mechanical and optical components. The use of a computer allows fast and easy measurements. Due to its simplicity, this technique can also be used to measure roughness in continuous production processes.

**THEORY**

The recognition, location, and description of 3D objects from natural light images are often difficult to obtain. In this paper we put forward an approach based on 3D analytical geometry. First we start with two-dimensional analytic geometry to recognize symmetric objects like cone, cylinders, spheres, ellipsoids etc. After obtaining a set of ten coefficients from the explicit representation of quadrics, a series of 2D curves are obtained from the intersection of planes at various orientations with surfaces. It is observed that only two planes are sufficient to generate a unique set of curves distinguishing each object from the other.

**3D Discriminant**

A 3D approach of classification and reduction of quadrics, which also looks into the various invariants of the quadric from translations and rotation of 3D objects.

$$F(x,y,z)=ax^2+by^2+cz^2+2fyz+2gzx+2hxy+2px+2qy+ 2rz+d =0 \text{-----(1)}$$

Define two matrices namely D and Δ such that

$$D = \begin{bmatrix} a & h & g & p \\ h & b & f & q \\ g & f & c & r \\ p & q & r & d \end{bmatrix}$$

$$\Delta = \begin{bmatrix} a & h & g \\ h & b & f \\ g & f & c \end{bmatrix}$$

Let A, B, C, D, E, F, G,H, P,Q and R denotes the cofactors of a, b, c, d, f, g, h, p,q and r respectively in the determinant Δ and α, β γ φ,ξ denote the cofactors of a, b, c, f, g, h respectively in determinant D. Here, I = a+b+c, J=α+β+γ, D and Δ the determinants are invariant for any general coordinate transformation. Combining these four invariants a further set of three absolute invariants, I J/D, I2/D and I D/ is also obtained.

**Surface Characterization**

Consider the equation of an ellipsoid (spheroid) resting on a plane parallel to yz plane and its axis of revolution parallel to y-axis then equation (1) reduces to

$$\frac{x^2 + p/a}{1/a} + \frac{y^2 + q/b}{1/b} + \frac{z^2 + r/a}{1/a} - 1 = 0,$$

only if  $d = p^2/a + q^2/b + r^2/a - 1, a > 0, b > 0.$

Consider the intersection of the ellipsoid with plane 1, i.e.

$$x=k, \text{ where } -p/a + 1/a < k < -p/a + 1/a$$

Then 
$$\frac{y^2 + q/b z^2}{1/b - \left[ \frac{ak+p}{ab} \right]^2} + \frac{z^2 + r/a^2}{1/a - \left[ \frac{ak+p}{a} \right]^2} - 1 = 0$$
 which is the equation of an ellipse.

**Conic Kernel:**

There are several equivalent coordinates to represent 3D orientation. They differ in the number and form of orientation variables. For example, a 2D polar angle and an implicit elevations angle (between the polar radius and z-coordinate) are used together to describe 3D orientation in the cylindrical coordinates, while three directional angles, (i.e. three angles between three Cartesian coordinate [3-4]). For orientation analysis, we believe that the orientation variables should be as small as possible to alleviate the complexity of indexing and visualization. Thus, we choose the spherical coordinates in which only two angles (azimuth and elevation) are needed to represent 3D representation.

The input data for plane analysis and measurement can be either the local image derivatives space (i.e. a space coordinated by partial derivatives of images with respect to different axes). They are the same for filtering purpose. For simplicity, we use the same representation

$I(x, y, z)$  for both kinds of input data. Here we assume that  $I(x, y, z)$  is correctly obtained for every  $(x, y, z)$ . Thus, the error in obtaining image derivatives or spectrum is not considered. For orientation analysis we start by computing a local spherical mapping on the input data through

Cartesian coordinate to polar coordinate by following steps

$$I(x, y, z) \rightarrow (r, \theta, \phi)$$

$$\text{where } r = \sqrt{x^2 + y^2 + z^2}, \theta = \arctan(y/x), \phi = \arctan(z/\sqrt{x^2 + y^2}) \quad (2)$$

In order to have fine orientation resolution we use conic kernels with small angular support to sample the orientation space locally. These kernels are radial-angular separable. A conic

kernel centered at  $(\theta_i, \phi_j)$  reads

$$k_{(\theta_i, \phi_j)}(r, \theta) = \frac{G_{\theta_i, \phi_j}(\theta, \phi)}{N_{R_{min}, R_{max}}(r)}$$

Where  $N_{R_{max}, R_{min}}^{\theta_i, \phi_j}(r)$  is a compensation function along the radial direction? First we focus on the angular part of the kernel, which is 2D Gaussian function [4-5] in  $(\theta, \phi)$ -space

$$G(\theta, \phi) = \frac{1}{2\pi\sigma^2} \exp\left(-\frac{(\theta - \theta_i)^2 + (\phi - \phi_j)^2}{2\sigma^2}\right) \quad (3)$$

As the azimuth angle  $\theta$  is periodic, we define a  $\mu(\cdot)$  to represent the minimal circular difference between  $\theta$  and  $\theta_i$  ( $\theta, \theta_i \in [0^\circ, 360^\circ]$ ),

$$\mu(\theta, \theta_i) = \min(|\theta - \theta_i|, |\theta - \theta_i - 360^\circ|, |\theta_i - \theta + 360^\circ|)$$

Conic Kernel response to 3D planes

In the 3D coordinate systems, a plane passing through the origin (0, 0, and 0) with a unit normal vector

$$N = (n_1, n_2, n_3)^T \text{ reads } x n_1 + y n_2 + z n_3 = 0$$

In order to represent a plane with  $(\theta, \phi)$ , we convert the Cartesian coordinates into spherical coordinates

$$(x, y, z) \rightarrow (r, \theta, \phi) \text{ and } (n_1, n_2, n_3) \rightarrow (1, \theta_n, \phi_n)$$

After dropping out (r) we obtain an equation with variable  $\theta$  and  $\phi$

$$\cos(\phi) \cos(\phi_n) \cos(\theta - \theta_n) + \sin(\phi) \sin(\phi_n) = 0$$

After horizontal and vertical planes with normal parallel to the co-ordinate axes, their corresponding representations in the  $(\theta, \phi)$  space are straight lines. In 3D analysis, we usually encounter titled planes which turn into harmonic curves with different amplitudes and phases in the  $(\theta, \phi)$ -space. The normal vector of each plane i.e.  $(\theta_n, \phi_n)$  is related to the extremepoint  $(\theta_m, \phi_m)$  on corresponding curve as follows

$$\theta_n = \theta_m + 180^\circ$$

$$\phi_n = 90^\circ - \phi_m$$

The titled phase's parameters (u, v) can then be estimated using  $(\theta_n, \phi_n)$

$$u = \cos(\theta_n) \cot(\phi_n)$$

$$v = \sin(\theta_n) \cot(\phi_n)$$

Further, each harmonic curve has two zero-crossing points on the axes with a distance of 180 and  $\theta_n$  lies exactly in the middle of two zero-crossing points [5-6].

The extra geometry constraint is very useful in determining the number of points. Further, each harmonic curve has two zero-crossing points on the  $\theta$  axis with a distance of 180 and  $\theta_n$  lies exactly in the middle of these two zero-crossing points. This extra geometry constraint is very useful in determining the number of planes automatically as well as in obtaining reasonable initial values of plane parameters. In practice, we obtain a set of points in the  $(\theta, \phi)$ -space. Extracting the parameters  $(\theta_n, \phi_n)$  from these points is then a standard fitting problem. For a simple curve, least square estimation is applicable [6].

## DESCRIPTION OF THE METHOD

The system for image acquisition is developed around National instruments image Acquisition Card, PCI 1408, installed on the Pentium III. This card can acquire the monochrome images with a maximum transfer rate of 132 M bytes/sec on 32 bit wide bus.

Image grabbing window is configured to acquire the image size 640 x 480 and pixel depth of 8 bits. The image is transferred from the camera to the computer at frame rate 30 frames per second. To achieve optimum results the roughness standard under study was illuminated from two different angles. The image was recorded by Pulnix TMC-76 CCD camera and image acquisition system. The image was stored in the two dimensional array.

Discrete wavelet transform is used to analyze the acquired image. The two-dimensional wavelet transform decomposes the image in horizontal, vertical, and diagonal components at different level of intensities containing texture information content. The processing is made through Labview 5.1 software and Matlab 5.2. Standard roughness sample is analyzed by using machine vision system described above and Symlet wavelet transform.

### Determination of the Exterior Orientation Elements

The bundle adjustment is based on the collinear condition, which refers to the perspective center of a camera, the points on the photograph, and the points in the object space being aligned in the bundle of rays. Rotation elements and the perspective center position of camera at the moment of exposure ( $X_0, Y_0, Z_0$ ) resulted from the least square method.

In this paper, the exterior orientation elements of digital images acquired by the CCD camera are not calibration data, so the interior and the exterior orientation elements were resulted from the bundle adjustment using the additional parameters of principal displacement and focal length.

For reliability evaluation of resulting exterior orientation elements, space coordinates of check points in each object space are computed by the bundle adjustment.

The accuracy of the computed positions is evaluated from residual errors and computed positions by the bundle adjustment.

Table 1. 3D ground coordinates of the check points in digital images acquired by the ccd camera (unit : mm)

Focal length	X		Y		Z	
	Bundle	Additional bundle	Bundle	Additional bundle	Bundle	Additional bundle
35 mm	0.259	0.227	0.285	0.193	0.250	0.242
70 mm	0.150	0.104	0.124	0.110	0.159	0.156

As shown in Table 1, RMS of images with 70 mm focal length is less than the case of 35 mm, and the additional bundle adjustment gives higher accuracy than the bundle adjustment. So, in this case, we just used digital images of the reference surface acquired by the 70 mm focal length of ccd camera.

Auto matching for the acquisition of object space coordinates is commonly used in area-based matching method using the maximum correlation coefficient, which is computed based on the cross-correlation function, and this method was used in this paper.

Thus, in the determination of matching size, after conjugate points determined to have 20 pixel intervals using geometrical relation equation in the targets of between left and right images, the determined conjugate points are used as control points for matching.

Search size fixed as 45 x 45 in the control points surrounding, and averages of the maximum correlation coefficient of each window size from 7 x 7 to 21 x 21 are calculated by matching, so that 17 x 17 window and 45 x 45 search are the proper sizes for matching as shown in Table 2.

Table 2. Average correlation coefficients of each window size.

Size	7	9	11	13	15	17	19	21
Ave.	0.753	0.772	0.832	0.881	0.883	0.888	0.885	0.885

After all the points of each sample area were matched using the resulted matching size, we obtained conjugate points of the sub-pixel unit.

### Determination of the Three Dimensional Positions

Object coordinates were generated by applying the space intersection theory, where conjugate points are resulted by matching, and exterior orientation elements are obtained by the calibration process of systematic error.

### ERRORS IN MEASUREMENT:

As with any optical technique, a number of error sources degrade the accuracy of measurement.

When combining together multiple topography maps, limiting the sources of these errors becomes especially important because the errors magnify as multiple measurements are introduced.

Therefore we need to consider the error sources by this process.

Following are the errors which may influence the uncertainty in measurement:

1. Objective distortion and aberrations.
2. Magnifications.
3. Pixel aspect ratio.
4. Error of the measurement technique.
5. Detector/array nonlinearity.
6. Vibrations.
7. Errors due to defocus.
8. System noise.

### MEASUREMENT UNCERTAINTY IN ROUGHNESS MEASUREMENT

In roughness measurement a profile of the surface of a given work piece is measured by sampling. Thus the measured is represented by a vector of data. Consequently these data are

accompanied by a covariance matrix, in order to have the complete information of the measurement process.

Due to the uniformity of the measurement process, each data point of the input data vector is expected to be measured with same measurement uncertainty. Thus all entries in the diagonal of the covariance matrix are the same. If there is no knowledge about the correlation of the measured input data, then, according to GUM [1], the covariances have to be set to zero. In this case the covariance matrix of the measured input data is simply a constant diagonal matrix. However, even in this very simple case it will be shown that the covariance matrix of the filtered data is a full matrix with no zero entries. This is due to the fact that the filtration process always causes a correlation between the data points.



Fig. 1(a)Originalimage

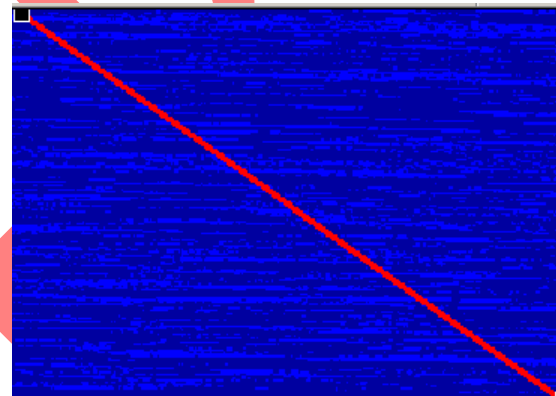


Fig. 2.a Phase structure of the surface.



Fig. 1(b) 3D Profilometry showing the structure

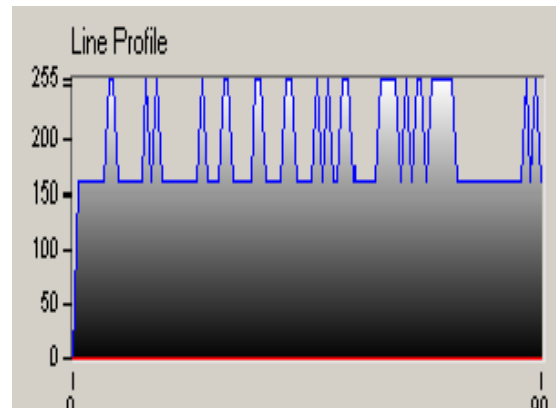


Fig 2.b Lineprofile

The line profile is taken across two points. The line profile is shown in fig.2.b.

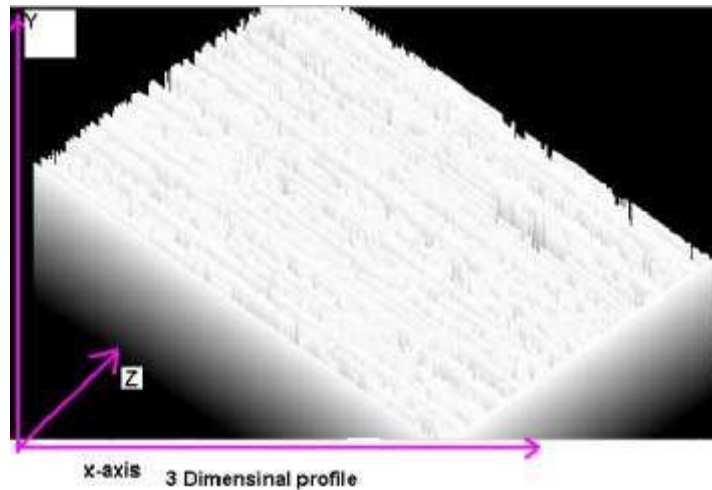


Fig3.a 3 dimensional profile after phase mapped.

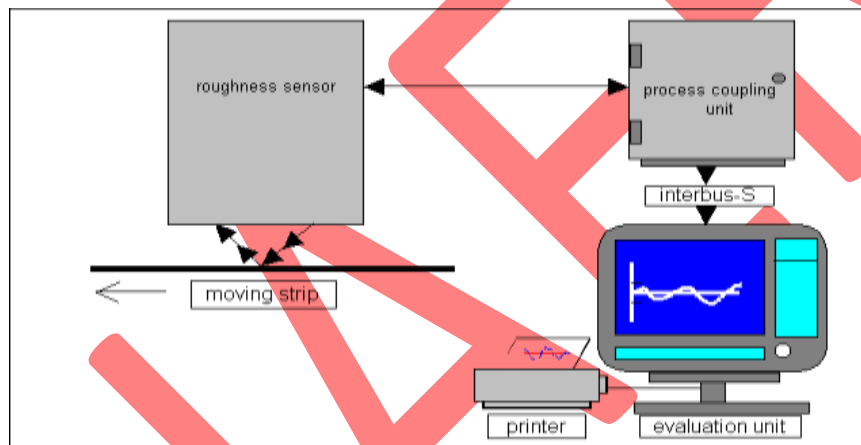


Fig 3.b: Schematic arrangement of process

The scale length in z-axis is of 110mm. It can detect and shows the measurement if the surface variation is upto 110mm approx.. The above figure shows how a small structure is either aligned or misaligned in micro level.

## COMPARISONS AND ANALYSIS

Surface roughness from the reference plane and the reference surface to all points in the sample area were computed with the proposed method in this paper.

In order to evaluate measurement-processing capability of the proposed system resultant values of a ccd camera were compared with the resultant values of surface roughness obtained by using standard contact type perthometer model6SP6.

Sample areas of digital images acquired by camera evaluated the same areas as did perthometer model 6SP6. Also, the three – dimensional position of each sample area was computed by applying the space intersection theory, where conjugate points resulting from



matching are used for all pixels in the sample area images. Surface roughness is computed with application of mentioned reference plane and reference surface equation using the resulting three – dimensional positions information.

*Table 3. Average of normal distance between the sample points and the reference surface*

Camera	CCD CAMERA		Perthometer
Reference surface Sample area	Surface	Plane	Plane
Sample 1	0.122	0.093	0.051
Sample 2	0.092	0.085	0.060

The average of surface roughness from the CCD camera shows inaccurate results with approximately 0.03 mm greater values than those of traditional method

The reason for this result is that a digital camera is a nonmetric camera without calibration data and resolution by the CCD sensor is fixed as 1524 x 1012 pixel, and pixel space of CCD arrangement is not constant.

## RESULTS AND DISCUSSIONS

Three- dimension measurement techniques and parameters are well understood and widely adopted for characterizing surface finish and performance. Nevertheless, in many application two- dimensional (2D) parameters are the only parameters specified for controlling surface quality. In most cases, average roughness (Ra) is the parameter specified.

This paper explores why 2D parameters continue to be used and, what is more important, it describe how 3D parameters can be measured to provide greater insight into surface finish and performance It also includes two cases in which 3D parameters have helped in the design and development of high performancesurfaces.

The roughness standards are made of hardened stainless steel of dimensions 40 mm x 20 mm x 10 mm. They have irregularly profile which repeated every 4 mm in longitudinal direction of the specimen. Normal to the measuring direction of the specimen, the grooves on the measuring faces are constant in the form of profile

The nominal values of the set 3 roughness standards in  $\mu\text{m}$  are:

Ra: 0, 2 0, 5 1,5

Rz : 1,5 3 8,5

The standards deviation calculated from 12 measurements is:  $s \leq 6\%$  of Ra and Rz.

## CONCLUSION

Important measuring tasks in dimensional metrology have been identified in the non-contact optical systems. For this subject, solutions have been presented, which make use of optical techniques. Initial results are quite satisfactory and show the 3D-orientation measurement.

More comparable calibration of this method against standard method is in progress. The results obtained by image processing system are compared with the results obtained using optical techniques.

It is seen that repeatability in our scheme is comparable with the standard method

1. Standard surface roughness from the reference plane and surface can be measured accurately with less than  $\pm 0.1\mu\text{m}$  errors, after applying the filtering scheme.
2. A primary window operating roughness measurement system can be constructed by using a digital camera and Microsoft Visual Basic 6.0 in Window environment for real time processing.

Results of this study may be applied to industrial inspection and measurement of mechanical parts in high precision.

## REFERENCES

1. A. Asundi and W. Zhou, "Unified calibration technique and its applications in optical triangular profilometry," *Appl. Opt.*, 38(16), 3556-3561(1999).
2. Y. Y. Hung, L Lin, H. M. Shang, and B. G. Park, "Practical three dimensional computer vision techniques for full-field surface measurement," *Opt. Eng.*, Vol. 39(1), Jan2009.
3. S. Kakunai, K. Iwata, S. Saitoh, and T. Sakamoto, "Profile measurement by two-pitch grating projection," *Int. J. Jpn. Soc. Precis. Eng.*, 588, 877-882(1992).
4. B.N. Taylor and C.E. Kuyatt, "Guidelines for evaluating and expressing the uncertainty of NIST measurement results," *Opt. Eng.*, Vol. 39(1), Jan2000.
5. Guide to the Expression of Uncertainty in measurement, international organization for Standardization, Geneva, Switzerland(1993).
6. B.N. Taylor and C.E. Kuyatt, Guidelines for Evaluating and Expressing the Uncertainty of NSIT Measurement Results, Technical, Note 1297, 1994 Edition, National Institute of Standards and Technology(1994).
7. Fraser, C.S. and Shortis M.R., 1995, Metric Exploitation of Still Video Imagery, *Photogrammetric Record*, 15(85): 107 –122.
8. KODAK, 1997, Professional Digital Cameras User's Manual, Estman Kodak Company, U.S.A.: 1-1-8-74.
9. Lichti, D.D., Chapman, M.A., Boyd, S.K. Ronsky, J.L., 1997, Digital Photogrammetric Measurement of Knee Joint Surfaces, Technical Papers of 1997 ACSM/ASPRS Annual